L. Marot et al.

Optical Coatings as Mirrors for Optical Diagnostics

Optical coatings as mirrors for optical diagnostics

L. Marot[a], G. Arnoux[b], A. Huber[c], V. Huber[d], Ph. Mertens[c], G. Sergienko[c], E. Meyer[a], and JET Contributors[†]

EUROfusion Consortium, JET, Culham Science Centre, Abingdon, OX14 3DB, UK

[a]*Department of Physics, University of Basel, Klingelbergstrasse 82 4056, Basel, Switzerland.*
[b]*CCFE, Culham Science Centre, Abingdon, Oxon, OX14 3DB, UK.*
[c]*Forschungszentrum Jülich GmbH, Institut für Energie- und Klimaforschung - Plasmaphysik, 52425 Jülich, Germany*
[d]*Jülich Supercomputing Centre, Research Centre Jülich, 52425 Jülich, Germany*
[†] *See the Appendix of F. Romanelli et al., Proceedings of the 25th IAEA Fusion Energy Conference 2014, Saint Petersburg, Russia*

Abstract

The aim of this work was to provide a comprehensive insight concerning coated films which might be used for first mirrors in ITER. The influence of the mirror crystallite size has been addressed as well as the coating techniques to provide nanocrystalline films. Tests of coated mirrors both in laboratories and in tokamaks are reviewed. For the tokamak tests a wide angle camera system has been installed in JET-ILW which is composed of a mirror box with 3 stainless steel mirrors coated with rhodium viewing the torus through a conically shaped aperture. The system delivered the required image quality for plasma monitoring and wall protection. No or insignificant degradation of the optical transmittance has been observed during the C33 experimental campaign in 2014 with about 3000 plasma pulses in different magnetic field configurations.

1. Introduction

In current fusion experiments the plasma is often viewed directly, which will not be possible in future tokamaks (e.g. ITER) due to the high level of neutron radiation expected. Therefore, metallic mirrors are foreseen to play a key role in guiding the plasma light towards the optical diagnostics. As these so-called first mirrors (FM) directly view the plasma, they will be subjected to a harsh environment of particle fluxes due to charge exchange neutrals and neutrons, as well as UV, x-ray and gamma radiation [1].

Molybdenum (Mo) and rhodium (Rh) are two important candidate materials for FM, especially in ITER. Molybdenum, due to its low sputtering yield, is more advantageous under erosion conditions [2]. Rhodium, on the other hand, provides a better reflectivity (between 70-80%) in the visible range [3] as well as near-infrared and infrared ranges (around 85% at 1μm). Rh has also low chemical reactivity, preventing oxide and carbide formation [4,5]. In the case of polycrystalline mirrors composed of many grains with random orientation of faces,

the sputtering yield can vary strongly over the material surface depending on the crystallographic plane of each individual grain and its orientation with respect to the incoming particle flux [6,7,8]. It is also important to keep the surface relief pattern i.e. the roughness of a polycrystalline mirror small compared to the wavelength of the reflected light in order to minimize the effect of diffuse reflection on the measurements. Generally, this indicates that the mirrors must have small grain sizes and preferably similar crystal orientation to be homogeneously sputtered. These requirements can be fulfilled, for instance, by using a single crystal or by coating the surface with nanometer-size crystallites. Moreover, test of amorphous metal alloy mirrors were carried out under ion bombardment, even though these mirrors have no crystalline structure. The initial optical quality under long-term sputtering was not maintained [9, 10]. Due to technological difficulties in producing large size Mo single crystals, coating might be considered as an alternative.

2. Realisation of coated mirrors

The preparation of such coated mirrors was reported by magnetron sputtering [3,11], evaporation [12] and pulsed laser deposition (PLD) [13-15] technique for Rh, Mo and W coatings. Silver and aluminum coatings with a thick protective dielectric layer with low rate of sputtering and chemical modification (Al_2O_3, ZrO_2) were also investigated [16,17]. The ZrO_2 films deposited at room temperature were found to have good homogeneity without microcrystalline inclusions. The observed needle-like pores in ZrO_2 may provide a path for hydrogen transport through the film, inhibiting its accumulation at the oxide-metal interfaces and therefore preventing blister formation [17]. Several proven techniques offer the possibility to produce coated mirrors at least on a laboratory size (tens of centimeters) with nanometric crystallites and a dense structure. The peculiar PLD capability to tailor film structure at the nanoscale gives the possibility to deposit low roughness Rh films with a wide variety of structures (polycrystalline, highly oriented and amorphous) and morphologies. This technique allow to deposit planar and homogeneous Rh films effectively suppressing surface defects on areas of the order of $10\ cm^2$ with a satisfactory specular reflectivity. For all the techniques previously mentioned the optical properties of the coated films are similar to the theoretical one. Industrial-type ITER FM mock-ups prepared by magnetron sputtering have already been manufactured [18]. A total of eight cooled full-scale ITER mirrors of 109 mm diameter have been manufactured by magnetron sputtering technique. The polishing quality achieved is characterized by a flatness error lower than 0.1 μm root mean square and roughness lower than 2 nm. The spectral reflectance of the coating deposited by magnetron sputtering reaches the theoretical values for both the molybdenum and rhodium layers. The spatial homogeneity of the reflectance over 100 mm in diameter is better than 4 %. However, the mirror flatness error has significantly increased due to the coating process, which shows that sample and/or target rotation during deposition is needed.

3. Laboratory tests

Mo and Rh coated mirrors were tested in laboratory in terms of their mechanical properties i.e. adhesion to the substrate [14,19], chemical reactivity towards typical tokamak impurities (like oxygen or carbon from residual gas fractions with partial pressure $< 5 \times 10^{-8}$ mbar or elements eroded from the first wall (like tungsten) [4,5,20-22]. It appeared that the adhesion increased with increasing substrate hardness and increasing deposition temperature for the magnetron deposition technique. For PLD the highly-oriented polycrystalline film structure guarantees the best adhesion to the substrate while a higher cohesion is achieved in the amorphous-like film [14]. Ion bombardment and especially deuterium plasma exposures were performed for Mo and Rh mirrors [23-25]. For example, 200 eV D^+ exposures of coated molybdenum mirrors causes no significant mechanical damage such as blistering of the coating or increase of the surface roughness. The drop of reflectivity may be explained with the complex permittivity $\varepsilon = \varepsilon 1 + i\varepsilon 2$. The smaller decrease in $\varepsilon 1$ (the real part of the permittivity) of exposed mirrors with increasing wavelength is attributed to a shorter intraband relaxation time compared with virgin mirrors. This suggests enhanced light scattering, which can be attributed to surface and grain boundary scattering, defects, and impurity scattering. Since the diffuse reflectivity measured by the spectrophotometer does not increase after any of the exposures, surface and grain boundary scattering are negligible. The lower amplitude of $\varepsilon 2$ (the imaginary part of the permittivity) of exposed mirrors compared with virgin mirrors for lower wavelengths is attributed to weaker optical absorption associated with the interband transitions. This is also due to a higher concentration of deuterium and deuterium induced defect in the subsurface layers of molybdenum mirrors as a result of implantation [25]. Mo coatings will remain functional in most of the cases in ITER, however higher energy of impinging charge exchange neutrals or lower surface temperature of the coatings can lead to gradual or sudden failure of the coatings [26]. Rh mirrors exposed to D_2 plasma show a drop in the reflectivity which can be associated with a formation of a subsurface rhodium deuteride (RhD_x, $x \leq 2$), which has optical constants different to those of Rh [22]. Crystal structure and morphology of rhodium films strongly affect the change of the specular reflectivity during exposure to deuterium plasmas [24]. In particular, films with few nm crystallite size and granular-like morphology prevent the reflectivity degradation, probably as a consequence of the inhibition of rhodium deuteride sub-superficial layer formation. Moreover, as reported mock ups including water cooling were realised [18] and recently exposed to H_2/Ar (10%) plasma in the Magnum-PSI linear plasma device [27]. Roughening of the coated mirror surface is flux and temperature dependent i.e. at RT implanted hydrogen cannot easily diffuse along the grain boundaries towards the surface. This increases the dynamic hydrogen inventory in the layer and thus its tendency to blister. Mo mock ups of coated mirrors exposed in Magnum-PSI show a high diffuse reflectivity after H_2, Ar plasma inducing a specular reflectivity loss at 500 nm higher than 60%. In case of water

cooled mock ups with 5 µm Rh films, at a flux of 3×10^{23} m^{-2}/s the plasma generates a high stress in the film leading to a delamination which is not seen for 1 µm Rh films. This is explained by the higher compressive energy stored in the thicker film which leads to failure under ion flux exposure directly for the first plasma exposure.

4. Tokamak exposures

Tests were carried out in TEXTOR [3, 28], DIII-D [29], JET-C [30, 31] and JET-ILW [32] showing no critical failure of the coated mirrors like delamination or strong degradation of the optical properties. For example in TEXTOR for Rh coated mirror exposure, the film survived under erosion conditions although the reflectivity was decreased by 8% at 250 nm after exposure [3]. For another exposure of a Mo coated mirror, a 2.5% degradation of reflectivity in the UV range was noticed under erosion after an exposure fluence of 1.4×10^{25} ions/m^2. Mostly, Rh and Mo coated mirrors were investigated, also in JETduring the 2013-2014 campaign. In previous studies in the JET-C wall configuration, Rh coatings with an initial reflectivity 30% better than that of pure Mo survived the test without detachment, however, their post-exposure reflectivity was the same as that of the exposed Mo surfaces [30]. Results of JET-ILW mirrors exposure in the main chamber wall show for Rh mirror surfaces originally having very high reflectivity a significantly reduced performance (25% at 250 nm); reflectivity is now at a level typical for Mo polycrystalline mirrors in most of the spectral range under examination. For all materials degraded performance is observed in the entire spectral range (250-2500 nm), but the most significant decrease is in the UV range (250-400 nm) [32]. Despite these results no further experiments from the JET First Mirror Test were started in 2013 and 2014. However, optical systems using coated mirrors for plasma monitoring and wall protection are used nowadays in JET-ILW; this last point is developed in the present paper including characterizations of these mirrors.

5. Wide angle viewing system at JET-ILW

After the previous examples of tokamak tests of coated mirrors it was important to demonstrate a complete optical diagnostic system operating in a metallic tokamak and especially at JET. During the JET-ILW shutdown a wide angle camera system has been installed [33]. The 2011-2012 campaigns exposure lasted 18.9 h in total with approximately 13.1 h of X-point operation and after that the mirrors were exposed also to 19 h in total with 12 h of X-point operation for the 2013-2014 campaigns. This system, composed of a mirror box with 3 stainless steel mirrors coated with Rh, is attached to the vacuum vessel wall on the low field side of the JET torus. The mirror system contains two branches, a lower and an upper branch. Each of the branches viewing half of the machine through a conically shaped aperture with a minor diameter of 3 mm. A 30° off-axis parabolic mirror with a focal length

of 50.8 mm creates an intermediate image of the object inside the box close to the surface of the next, flat mirror. The half images of the two branches are then combined on the camera sensor to form a full wide angle view image. The detailed description of the wide angle imaging system is given in [33]. A rhodium film (175 nm thick) was evaporated directly on polished flat stainless steel mirrors (60×40 mm). On the other hand, for the parabolic mirrors a 100 m amorphous electroless coating of a nickel-phosphorus alloy was used on the polished stainless steel surface as an interlayer to reduce the micro roughness of the surface after polishing and to allow accurate surface shaping. The characterisations of the films were carried out on witness samples (25 mm in diameter). The diffuse reflectivity was below 3% in the range 250-2500 nm and the specular reflectivity was similar to the reference one [3]. Reflectivity measurements were also performed at incidence angles of 40, 50, 60, 70 and 80° for perpendicular (s) and parallel (p) polarized light with a spectral ellipsometer SENTECH S 850, and are identical to the reference one (Fig 5 in reference 3). The reflectivity observed for a natural or unpolarized light, containing an equal mix of s and p-polarisations is given by the sum of Rs and Rp divided by 2. SEM observations show small crystallites (few tens of nm) typical for evaporated Rh films [12]. Chemical analyses of the surface by XPS after 6 hours annealing at 600 °C in air revealed a Rh metallic surface covered with adsorbed molecules (oxygen, carbon) and a thin rhodium oxide layer as described in our previous paper [3] but nothing else. No degradation of the optical reflectivity was observed after this annealing in contrary to Mo mirrors which oxidised in air [32] showing a reflectivity decrease of more than 10% in the visible range between the mirror production and JET installation. The system delivered the required image quality for JET plasma monitoring and wall protection.

For the 2013-2014 campaigns a new system, KL14, was installed in JET (Figure 1) using the lower left limiter guide tube. A mirror box identical to the previously described one is used and a new flat stainless steel mirror (165×80 mm) coated also with Rh was added to guide the optical beam (Figure 2). This system was also given the same measurements quality. Monitoring discharges with identical plasma shape and operational parameters have been regularly executed to document the change in the optical performance of the wide angle systems [34]. Figure 3 shows the time evolution of typical monitoring pulses: pulse #84570 directly after the installation of the new wide angle KL14 system and the pulse #87402 at the end of the experimental campaign. These L-mode pulses with an additional NBI-power of about 1.2 MW have been performed at $B_T \approx 2.0$ T, I_p=2.0 MA and safety factor q95=3.2. For precise control of the changes of the optical performance it is important to keep the radial outer gap (ROG) as well as the inner gap (RIG) constant. The gap is the distance between the plasma surface (LCFS=Last Closed Flux Surface) and the first wall. Figure 3 shows the same values of RIG and ROG for the analysed pulses indicating the identical plasma shape. The central line-integrated plasma density as well as the D_α emission in the outer divertor were also identical.

The wide angle view imaging system contains two CCD cameras, colour and monochrome cameras, each of it equipped with telephoto zoom lenses set to a focal length of 250 mm and 300 mm consequently. An unfiltered colour CCD camera provides video images for general plasma operation monitoring in the visible spectral range. Figure 4 shows images taken by the colour camera directly after installation of the wide angle KL14 video systems (#84570) and at the end of the experimental campaign (#87402). No visible degradation of the images has been observed. The composite RGB signal of the unfiltered colour CCD camera has been split into three colour channels: Red: 580-750 nm; Green: 475-570 nm; Blue: 430-480 nm. The colour channels have been compared for the mentioned two monitoring pulses (see Fig. 5). Figure 5 shows the comparison for three Region of the interest (ROI): ICRH antenna, Inner Wall Limiter, Upper dump plate. No or an insignificant degradation of the optical transmittance has been observed during one experimental campaign (about 3000 plasma pulses in different magnetic field configurations).

For both systems a detailed ex-situ optical characterisation of the mirrors is foreseen in the future.

6. Concluding remarks

Metallic coated mirrors were extensively studied for ITER's FM purpose concerning the manufacturing techniques, characterisations and laboratory tests. Thick coated Rh mock up delaminated at high flux exposure, which is a 1000-fold higher the D(T) incident fluxes (up to 10^{20} m^{-2}s^{-1}) that can be expected at the outer midplane wall of ITER [35], due to a high energy stored in the film. For an identical fluence but at a 100-fold lower flux level, tokamak tests in TEXTOR, DIII-D, JET-C and JET-ILW showed no critical failure of the coated mirrors like delamination or strong degradation of the optical properties. Two complete diagnostics using Rh coated mirrors i.e. wide angle viewing systems were installed in JET-ILW, they delivered the required image quality for plasma monitoring and wall protection.

References

[1] M. Walsh et al., "ITER Diagnostic Challenges," IEEEINPSS 24th Symposium on Fusion Engineering, 2011.

[2] J.N. Brooks et al., J. Nucl. Mater. 48 (2008) 045003

[3] L. Marot et al., Rev. Sci. Instrum. 78 (2007) 103507

[4] L. Marot et al., Surf. Sci. 602 (2008) 3375

[5] L. Marot et al., J. Nucl. Mater. 390-391 (2009) 1135

[6] A. Bardamid et al., Vacuum 58 (2000) 10.

[7] M. Wisse et al., Rev. Sci. Instrum. 83 (2012) 013509.

[8] V.S. Voitsenya et al., Nucl. Instrum. Methods B 302 (2013) 32.

[9] V.S. Voitsenya et al., Plasma Devices Oper. 17 (2009) 144.

[10] A.F. Bardamid et al., J. Alloy. Compd. 514 (2012) 189.

[11] L. Marot et al., Surf. Coat. Tech. 202 (2008) 2837.

[12] B. Eren et al., Fusion Eng. Des. 86 (2011) 2593.

[13] M. Passoni et al., J. Nucl. Mater. 404 (2010) 1.

[14] A. Uccello et al., J. Nucl. Mater. 432 (2013) 261.

[15] A. T. T. Mostako et al., Rev. Sci. Instrum. 82 (2011) 013101.

[16] A.G. Razdobarin et al., Fusion Eng. Des. 86 (2011) 1341

[17] E.E. Mukhin et al., Nucl. Fusion 52 (2012) 013017

[18] M, Joanny et al., IEEE Transactions on Plasma Science, 40 (2012) 692.

[19] L. Marot et al., Thin Solid Films 516 (2008) 7604.

[20] B. Eren et al., J. Nucl. Mat. 438 (2013) S852.

[21] B. Eren et al., Appl. Surf. Sci. 273 (2013) 94.

[22] L. Marot et al., J. Nucl. Mat. 415 (2011) S1203–S1205

[23] A.F. Bardamid et al., J. Nucl. Mater. 393 (2009) 473.

[24] A. Uccello et al., J. Nucl. Mat. 446 (2014) 106.

[25] B. Eren et al., Nucl. Fusion 51 (2011) 103025.

[26] B. Eren et al., Nucl. Fusion 53 (2013) 113013.

[27] L. Marot et al., "First Mirror mock ups exposed to H_2/Ar (10%) plasma in the Magnum-PSI linear plasma device" in preparation.

[28] M. Matveeva et al., Material choice for first ITER mirrors under erosion conditions, in: 37th EPS Conf. on Plasma Physics, Dublin Ireland, 2010. http://ocs.ciemat.es/EPS2010PAP/pdf/P2.105.pdf.

[29] L. Marot et al., Coated mirrors for ITER 13th ITPA Diagnostic Meeting, Chengdu 2007 https://portal.iter.org/departments/POP/ITPA/Diag/DIAG/Document%20Library/21/Marot.mirrors.pdf

[30] L. Marot et al., J. Nucl. Mater. 438 (2013) S1187.

[31] M. Rubel et al., Physica Scripta. T145 (2011) 014070

[32] D. Ivanova et al., Physica Scripta, T159 (2014) 014011

[33] M. Clever, et al., Fusion Eng. Des. 88 (2013) 1342–1346

[34] J.W. Coenen et al., Nucl. Fusion 53 (2013) 073043.

[35] V. Kotov et al., Fusion Eng. Des. 86 (2011) 1583–1586
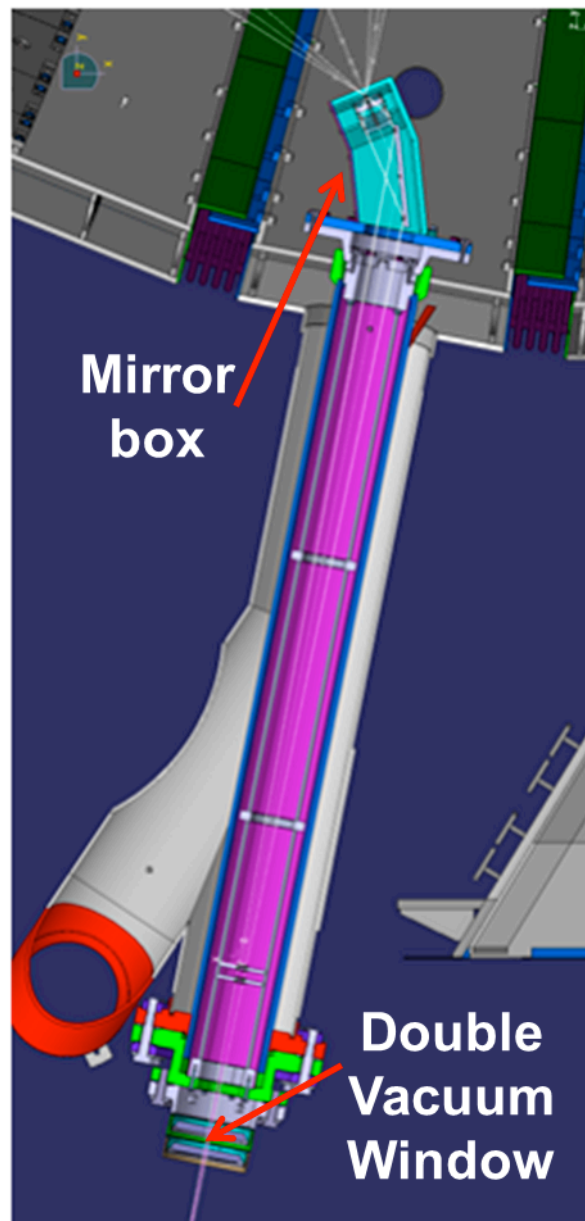
FIG 1

Figure 1: Schematic view from the top showing the optical path of the KL14 wide angle viewing system installed in the lower left limiter guide tube. The field of view of the system is tangential to the entire vessel including the wide outer poloidal limiter, re-ionisation plates, narrow outer poloidal limiter, lower hybrid antenna and inner wall guard limiters.
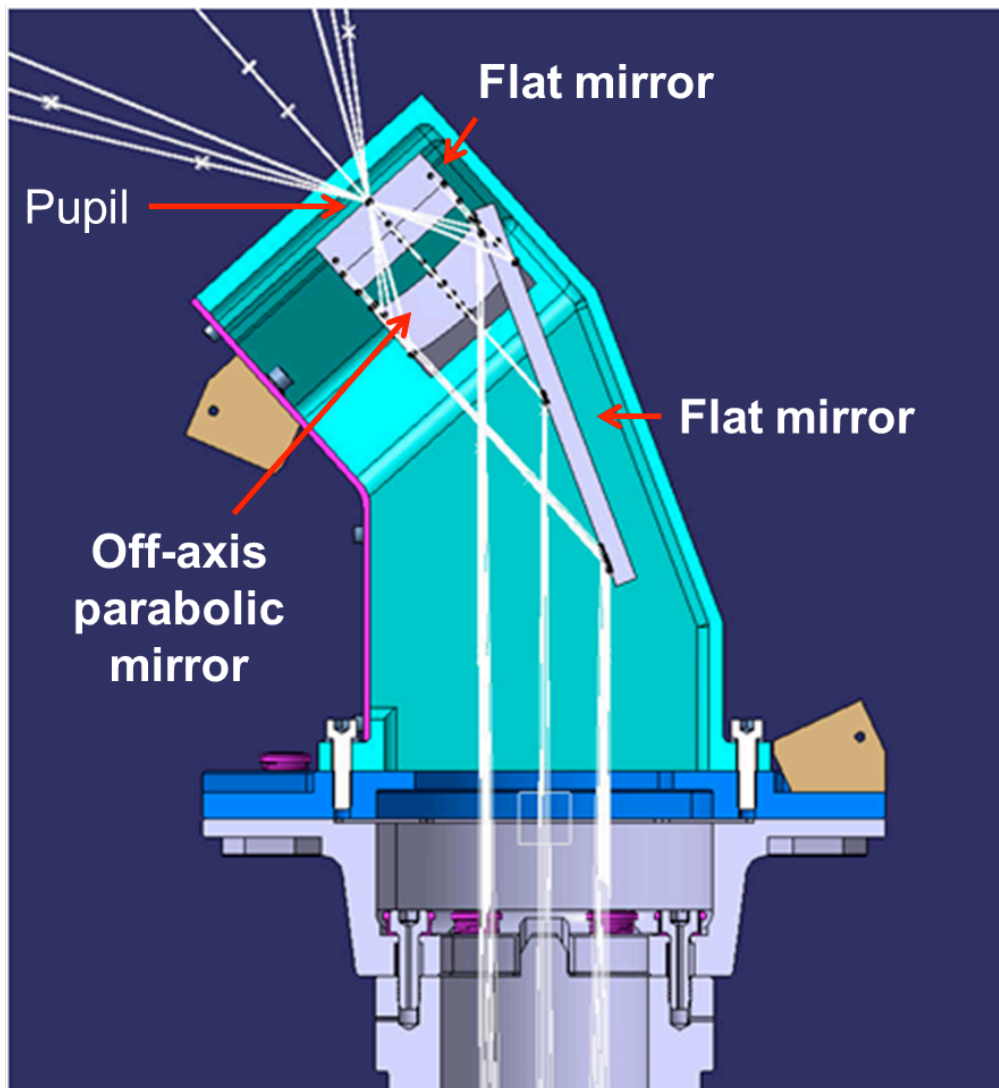
FIG 2

Figure 2: Top view of the mirror layout in the KL14 system including the optical path. The distance from the pupil to the plasma is around 20 centimetres, depending on the plasma configuration.
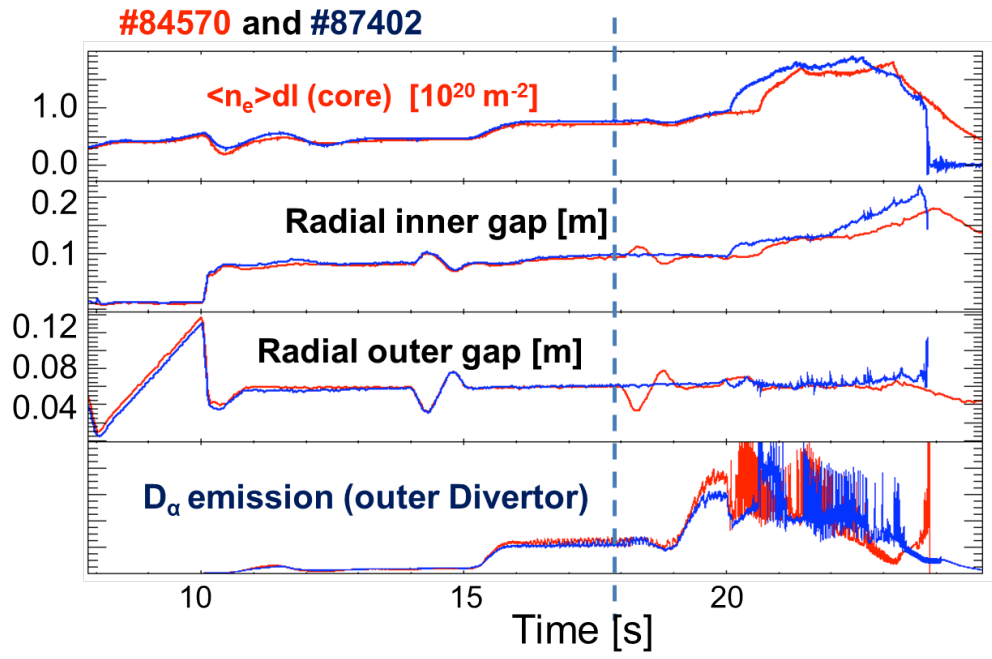
FIG 3

Figure 3: Time evolution of typical monitoring L-mode discharges which correspond to the next figure
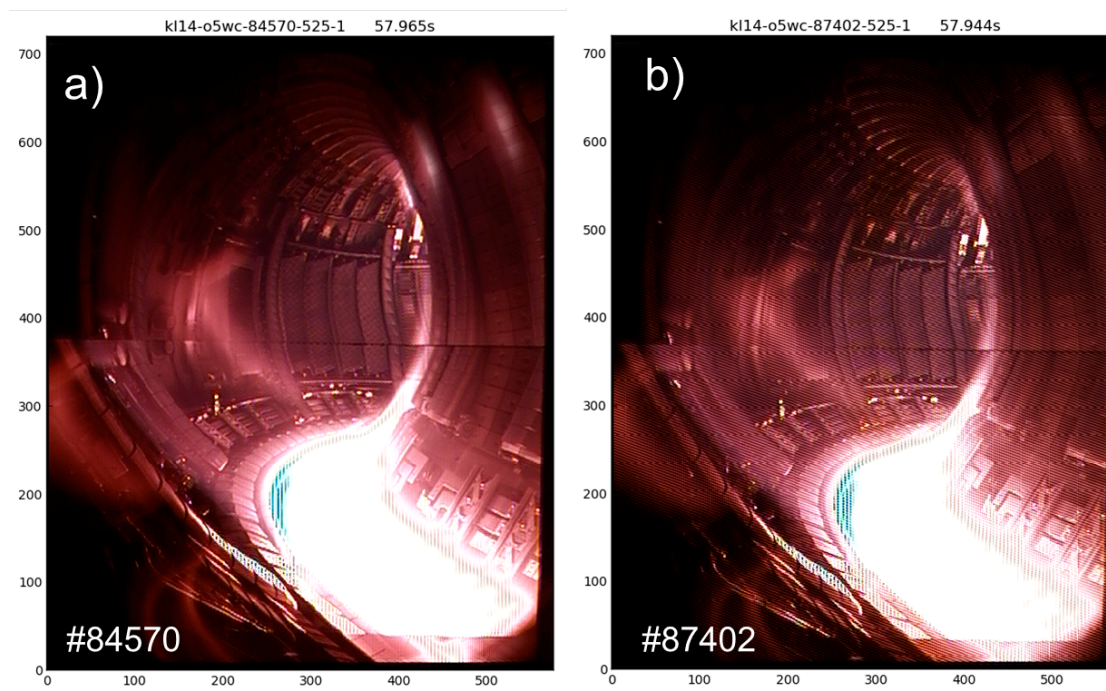
FIG 4

Figure 4: Two images taken by the colour cameras directly after the installation of the wide angle KL14 video systems (#84570) and at the end of the experimental campaign (#87402). Qualitatively no degradation of the picture can be observed, which is in line with results from quantitative comparisons at various key image areas (see figure 5).
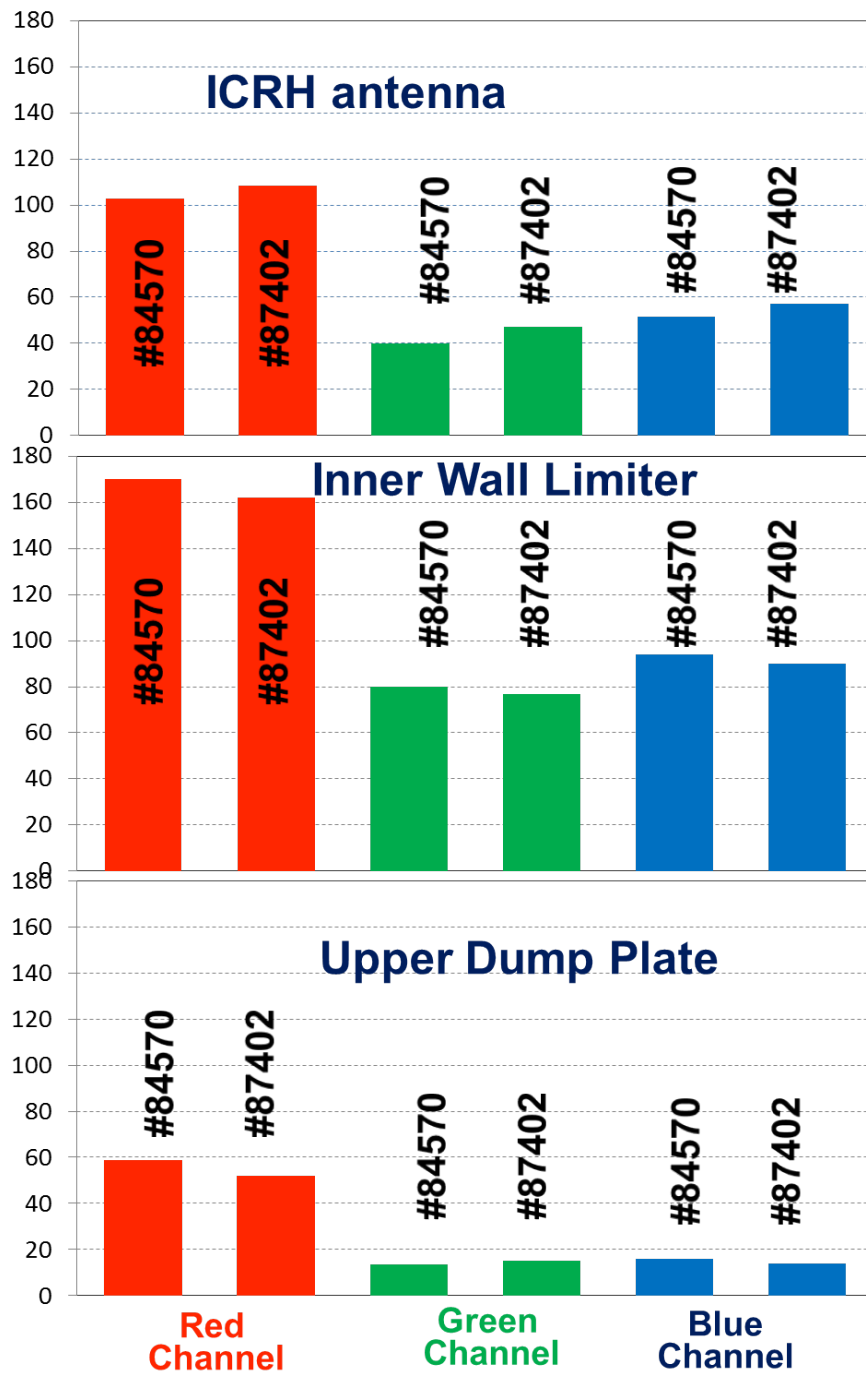
FIG 5

Figure 5: Comparison of the colours channels of the colour camera for two monitoring pulses: directly after the installation of the wide angle KL14 video systems (#84570) and at the end of the experimental campaign (#87402).